Rate Region and Achievable Rates of Full-Duplex Cognitive Radio NOMA Channels Under Imperfect Spectrum Sensing

Mohammad Ranjbar[1], Nghi H. Tran[1(✉)], Tutku Karacolak[2], and Shivakumar Sastry[1]

[1] Department of Electrical and Computer Engineering, University of Akron, Akron, OH, USA
{nghi.tran,ssastry}@uakron.edu
[2] School of Engineering and Computer Science, Washington State University Vancouver, Vancouver, USA
tutku.karacolak@wsu.edu

Abstract. This paper studies the rate region and the achievable rates of a non-orthogonal multi-access (NOMA) full-duplex (FD) cognitive radio (CR) channel in which multiple secondary users (SU) communicate to a base station under imperfect self-interference suppression (SIS) and spectrum sensing. Towards that goal, we first analyze the sensing performance, i.e., the probabilities of false alarm and miss-detection, of the considered NOMA FD CR channel under the assumption of non-time-slotted activity from the primary network. We use a Markov chain model to combine the sensing results under different sensing scenarios and derive the probability of collision between the primary and secondary networks under realistic imperfect spectrum sensing. Because of this sensing imperfection, the secondary channel is molded as a Gaussian-mixture (GM) channel. Due to the difficulty in obtaining the explicit expressions of the channel capacity and mutual information in GM, we propose new closed-form approximations of the rate region and the achievable rate for each of the users with arbitrarily small errors. These approximations are therefore helpful to analyze the rate region and to establish the achievable rates of the considered FD CR NOMA channel.

Keywords: Cognitive radio · Full-duplex · Gaussian-mixture interference · NOMA · Imperfect spectrum sensing

1 Introduction

Over the last decade, cognitive radio (CR) under the context of opportunistic spectrum access (OSA) has gained significant attention [7]. To date, most of the existing works under this line of research considered a single-user secondary network or a multi-user system but under orthogonal multiple access (OMA)

N.-S. Vo et al. (Eds.): INISCOM 2022, LNICST 444, pp. 3–19, 2022.
https://doi.org/10.1007/978-3-031-08878-0_1

schemes. While non-orthogonal multiple access (NOMA) schemes [3] provide significantly more benefits, the consideration of NOMA for CR poses significant challenges, especially under realistic conditions of imperfect sensing [15].

In CR with OSA, a SU periodically monitors the spectrum and opportunistically transmits over the spectrum holes. There has been an extensive literature on the analysis of OSA with regard to spectrum efficiency and throughput under the constraint of half-duplex (HD) communication, where an SU cannot sense and transmit simultaneously. With the recent development of full-duplex (FD) radio and self-interference suppression (SIS) [4,8], the integration of FD in CR has also been addressed [1,9]. For instance, the works in [1] considered the use of FD in a single-user CR that enables the SU to operate in different modes, such as transmit-and-sense (TS) and transmit-and-receive (TR) [1]. Such flexibility in operation helps improve spectrum sensing performance and/or throughput significantly. In [9], a "listen-and-talk" protocol based on FD was also proposed under TS framework for better spectrum utilization and sensing accuracy in CR.

In CR, even with FD capability, spectrum sensing is never perfect. When SU fails to detect the presence of the PU activity, miss-detection occurs, and both SU and PU suffer from interference. Under the practical assumption of finite input PU signals, it has been shown that the aggregate noise plus interference in the SU channel is Gaussian-mixture (GM) [10], which poses more challenges in the analysis. It is because the non-Gaussian characteristic leads to a totally different link and network behavior as compared to the Gaussian counterpart [12,14]. In our recent work in [13], we have studied the energy efficiency of a FD CR system under such non-Gaussian aggregate interference. However, the results were only obtained for a single-user scenario. To our knowledge, there does not exist any previous work in the literature that addresses the sensing performance and the corresponding transmission rates of a multi-user FD CR network under non-Gaussian aggregate interference.

Motivated by the above discussions, this paper studies the rate region and the achievable rates of a NOMA FD CR channel in which SUs communicate to a secondary base station (SBS) under imperfect SIS and spectrum sensing. In the considered NOMA, the SBS decodes the signal for each user by performing successive interference cancellation (SIC) [2]. With their FD capability, SUs can sense the channel while transmitting. We first analyze the sensing performance, i.e., the probabilities of false alarm and miss-detection, of the considered NOMA FD CR channel under the assumption of non-time-slotted activity from the primary network. We use a Markov chain model to combine the sensing results under different sensing scenarios and derive the probability of collision between the primary and secondary networks. Under imperfect spectrum sensing, we show that secondary channel is modeled as a Gaussian-Mixture channel. We then analyze the rate region of the considered FD CR NOMA channel and establish the achievable rates. Due to the lack of explicit expressions of both channel capacity and mutual information in GM channels, we develop new closed-form approximations with an arbitrary small error of the rate region and the achievable rate for each of the users.

2 System Model

In this work, we consider a cognitive multiple access channel where N SUs opportunistically access the primary channel and communicate to a secondary base station (SBS). The SUs have SIS capability and they can work in FD mode. The quality of the SIS method at user i, $1 \leq i \leq N$, is represented by a zero-mean circularly symmetric Gaussian (CSCG) random variable $\boldsymbol{h}_{ii}$ with variance σ_{ii}^2, which is the ratio of residual self-interference to the self-interference before suppression. Moreover, it is assumed that SUs always have data to transmit, i.e., saturated traffic.

To detect the white spectrum and avoid collision with the PU, the SUs take the samples of the channel with sampling frequency f_s and make a decision about the PU activity every N_s samples. This results in a time-slotted traffic with slot length of $\tau_s = \frac{N_s}{f_s}$. The SUs then report their sensing results to SBS and SBS makes a cooperative decision on the PU activity status. The entire sensing procedure will be explained further in the next section. It should also be noted that the PU activity is considered as non-time slotted, i.e., the PU can change its status any time. To take it into consideration, we introduce two new random variables T_1 and T_0 to represent the ON and OFF duration of the PU, respectively. These two random variables follow the probability distributions $f_{T_1}(\cdot)$ and $f_{T_0}(\cdot)$ and means τ_1 and τ_0, respectively. By assuming that f_s is large enough, the PU state changes sufficiently slow, and we have $\tau_0 \gg \tau_s$ and $\tau_1 \gg \tau_s$.

2.1 Modes of Operation

With FD, the SUs can sense the channel and, simultaneously, transmit data. As a result, we can have two different modes of operation of SUs as follows:

1. *Sense-Only (SO)*: If the channel is sensed as busy, the SUs only sense the channel until the next sensing result.
2. *Transmit-Sense (TS)*: If the channel is sensed as idle, the SUs simultaneously transmit and sense for the next SU time slot.

2.2 Secondary Channels Under Imperfect Spectrum Sensing

In practice, sensing performance is characterized by probabilities of false alarm P_f and miss-detection P_m. With FD, these sensing performance metrics are affected by the quality of SIS, and they will be analyzed further in the subsequent sections. In the case of false alarm or correct detection in the presence of the PU signal, SUs do not transmit, and the received signal at the SBS $\boldsymbol{y}_r$ is either noise or noise plus interference from PU. Otherwise, all SUs will transmit. The input-output model of the SU channel can therefore be expressed as:

$$\boldsymbol{y}_r = \begin{cases} \sum_{j=1}^{N} \boldsymbol{h}_{jr}\boldsymbol{x}_j + \boldsymbol{u}_r, & H_0, \hat{H}_0 \\ \sum_{j=1}^{N} \boldsymbol{h}_{jr}\boldsymbol{x}_j + \boldsymbol{u}_r + \boldsymbol{w}, & H_1, \hat{H}_0 \end{cases}. \tag{1}$$

Here, H_0/H_1 denotes the hypothesis that the channel is free/busy while $\hat{H}_0/\hat{H}_1$ represents the hypothesis that the channel is sensed as idle/busy. For convenience, throughout the paper, we shall use sub-index 0 to indicate the PU, while sub-indices $1, 2, \ldots, N$ and sub-index r to refer to the N SUs and the SBS, respectively. Furthermore, in (1), $\boldsymbol{y}_r$ is the received signal at the SBS, $\boldsymbol{x}_j$ is the zero-mean transmitted signals from SU j with variance σ_j^2. $\boldsymbol{u}_r$ is the additive noise at the SBS, which is modeled as CSCG random variable with zero mean and variance $\sigma_{u_r}^2$. Also, $\boldsymbol{h}_{jr}$ is a zero-mean circularly symmetric fading coefficient between SU j and the SBS with variance σ_{jr}^2, and $\boldsymbol{w}$ is the PU interference at the SBS. It is clear that in the case of Gaussian $\boldsymbol{w}$, $\boldsymbol{u}_r + \alpha\boldsymbol{w}$ is a mixture of two Gaussian distributions. In a more realistic scenario, $\boldsymbol{w}$ and, hence, the aggregate noise plus interference are more accurately modeled as general GM random variables [11]. In this work, we adopt this model, and assume that $\boldsymbol{w}$ has the following PDF:

$$f_W(\boldsymbol{w}) = \sum_{i=1}^{p} \epsilon_i \mathcal{CN}(\boldsymbol{w}, 0, \sigma_{w,i}^2). \tag{2}$$

In (2), $\{\epsilon_i\}$ are the mixture probability with $\sum_{i=1}^{p} \epsilon_i = 1$, and $\mathcal{CN}(\boldsymbol{z}, \mu, \sigma^2)$ denotes a circularly symmetric complex Gaussian distribution with mean μ and variance per real dimension $\sigma^2/2$. Also, we assume all the links to be reciprocal, i.e., $\sigma_{ji}^2 = \sigma_{ij}^2$.

Given that, the model in (1) can be represented in an equivalent way as $\boldsymbol{y}_r = \beta \sum_{j=1}^{N} \boldsymbol{h}_{jr}\boldsymbol{x}_j + \boldsymbol{u}_r + \alpha\boldsymbol{w},$, where β and α are binary indicator random variables. Specifically, $\beta = 0$ corresponds to the event of sensing the channel as free and $\alpha = 1$ denotes the event that PU is active.

In the considered multi-user setup, the SBS can decode the signal for each SU by performing successive interference cancellation (SIC). To this end, it is essential to maintain the distinctness of the users' signals superimposed in the received signal $\boldsymbol{y}_r$. To apply SIC, the SBS should first setup a decoding order. Since each user experiences a different channel gain, the received signal power corresponding to the user with the largest $\sigma_{jr}^2\sigma_j^2$ is likely to be the strongest at the SBS. Without loss of generality, it is assumed that $\sigma_{1r}^2\sigma_1^2 \geq \sigma_{2r}^2\sigma_2^2 \geq \cdots \geq \sigma_{Nr}^2\sigma_N^2$. Having set up the decoding order, the SBS then decodes the first user signal by treating other signals as noise and then subtracts this decoded message from $\boldsymbol{y}_r$. In the next step, the second user signal is decoded from the modified received signal (without any interference from the first user) and the decoded signal is again removed by SIC. This procedure goes on until the last user signal is detected without any interference.

2.3 Achievable Rates

Assuming that the SBS has full knowledge of the channel gains $\vec{\boldsymbol{h}}_r = [\boldsymbol{h}_{1r}, \boldsymbol{h}_{2r}, \cdots, \boldsymbol{h}_{Nr}]$, the achievable rate at each user j for a given set of power

budget $\Sigma = \left[\sigma_1^2, \ldots, \sigma_N^2\right]$, is the average mutual information between the input signal and the received signal, which is

$$R_j(\Sigma) = \mathrm{E}_{\vec{\boldsymbol{h}}_r}\left[I\left(\boldsymbol{y}_r, \beta; \boldsymbol{x}_j \mid \vec{\boldsymbol{h}}_r\right)\right] = \mathrm{E}_{\vec{\boldsymbol{h}}_r}\left[I\left(\boldsymbol{y}_r; \boldsymbol{x}_j \mid \beta, \vec{\boldsymbol{h}}_r\right)\right] = P(\beta = 1)\,\mathrm{E}_{\vec{\boldsymbol{h}}_r}\left[I\left(\boldsymbol{y}_r; \boldsymbol{x}_j \mid \beta = 1, \vec{\boldsymbol{h}}_r\right)\right]. \tag{3}$$

For simplicity, let $\boldsymbol{y}_r^{\beta} = \boldsymbol{y}_r \mid \beta = 1$ and $\boldsymbol{z}_{\beta} = \boldsymbol{u} + (\alpha \mid \beta = 1)\,\boldsymbol{w}$. We then have $\boldsymbol{y}_r^{\beta} = \sum_{j=1}^{N} \boldsymbol{h}_{jr}\boldsymbol{x}_j + \boldsymbol{z}_{\beta}$, where $f_{Z_{\beta}}(\boldsymbol{z})$ can be defined as

$$P(\alpha = 0 \mid \beta = 1)\,\mathcal{CN}(\boldsymbol{z}, 0, \sigma_{u_r}^2) + P(\alpha = 1 \mid \beta = 1)\sum_{i=1}^{p} \epsilon_i \mathcal{CN}(\boldsymbol{z}, 0, \sigma_{w,i}^2 + \sigma_{u_r}^2)$$

$$= \sum_{i=1}^{p+1} \epsilon_{z,i}\mathcal{CN}(\boldsymbol{z}, 0, \sigma_{z,i}^2). \tag{4}$$

Therefore, $R_j(\Sigma) = P(\beta = 1)\,\mathrm{E}_{\vec{\boldsymbol{h}}_r}\left[I\left(\boldsymbol{y}_r^{\beta}; \boldsymbol{x}_j \mid \vec{\boldsymbol{h}}_r\right)\right]$. Here, it is worth mentioning that $\alpha = 1 \mid \beta = 1$ corresponds to the event that there is collision between PU and SU, while $\alpha = 0 \mid \beta = 1$ is the event that SUs transmit without collision and $P(\beta = 1) = P\left(\hat{H}_0\right)$.

3 Sensing Performance Metrics

In this section, we shall focus on the sensing performance by studying the binary indicator random variables α and β. As mentioned earlier, $\alpha = 1$ corresponds to the event that PU is active and $\beta = 1$ is the event that SU decides to transmit. These two random variables are related to the following probabilities:

$$1 - P(\alpha = 0 \mid \beta = 1) = P(\alpha = 1 \mid \beta = 1) = \text{Probability of Collision},$$

and

$$P(\beta = 1) = P\left(\hat{H}_0\right),$$

which are needed for the rate analysis.

Different from traditional HD CR, in the considered FD CR, the state of the system at each SU time slot depends on the sensing decision in the previous slot. Therefore, in this paper, we model the sensing decision status as a discrete-time Markov chain. To analyze this Markov chain, let P_{10} and P_{01} be the probabilities of PU going from ON to OFF and OFF to ON, respectively, during an SU slot, and they are given as $P_{10} = F_{\hat{T}_1}(\tau_s)$ and $P_{01} = F_{\hat{T}_0}(\tau_s)$. Because $\tau_0 \gg \tau_s$ and $\tau_1 \gg \tau_s$, it can be verified that P_{10} and P_{01} are small. Also, as PU activity is modeled as non-time slotted, we have two types of slots:

1. The slots in which the PU activity does not change.
2. The slots in which PU activity status changes.

It is then clear that the sensing performance in these two cases are different, and they need to be treated separately. For convenience, we shall use following notations:

1. P_f^j: The probability of false alarm while working at mode $j \in \{so, ts\}$ for slots in which PU activity status does not change.
2. P_m^j: The probability of miss-detection while working at mode $j \in \{so, ts\}$ for slots in which PU activity status does not change.
3. $P_f^{j_c}$: The probability of false alarm while working at mode $j \in \{so, ts\}$ for slots in which PU activity status changes.
4. $P_m^{j_c}$: The probability of miss-detection while working at mode $j \in \{so, ts\}$ for slots in which PU activity status changes.

We now model the sensing decision status at each decision instance as a discrete-time Markov chain with four different states as follows:

1. State H_{00} representing $\hat{H}_0$ and H_0.
2. State H_{01} representing $\hat{H}_0$ and H_1.
3. State H_{10} representing $\hat{H}_1$ and H_0.
4. State H_{11} representing $\hat{H}_1$ and H_1.

From P_{10} and P_{01} and the probabilities of false alarm and miss detection, we can obtain the state transition diagram of the sensing decision as in Fig. 1.

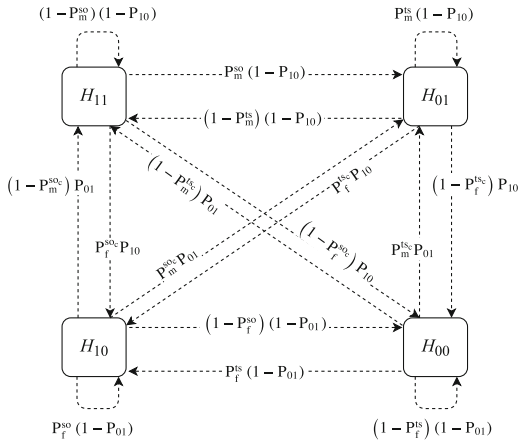

Fig. 1. The state transition diagram of the sensing status.

Given the proposed Markov chain, it is straightforward to verify that $P(\beta = 1) = P(H_{00}) + P(H_{01})$. In addition, we can find the collision probability and also the probability of collision-free transmission of SUs using this

Markov chain. To do that, let consider two scenarios in which collision happens in an SU slot:

1. When PU is present and SU fails to detect that the spectrum is occupied H_{01}. The probability of this scenario is the probability of H_{01}.
2. PU is not active and SU correctly senses the channel as free H_{00}. However, PU becomes active during SU transmission before the next sensing decision. The probability of this scenario is $P_{01}P(H_{00})$, which is relatively small.

Given these two scenarios, we can define the probability of collision during a time slot given that SU decides to transmit as

$$P_c = P(\alpha = 1 \mid \beta = 1) = \frac{P(H_{01}) + P_{01}P(H_{00})}{P(H_{00}) + P(H_{01})}. \tag{5}$$

Using the same argument, we can formulate the probability of collision-free transmission during a time slot as

$$P_{nc} = P(\alpha = 0 \mid \beta = 1) = \frac{(1 - P_{01})P(H_{00})}{P(H_{00}) + P(H_{01})} = 1 - P_c. \tag{6}$$

We now only need to find $P(H_{ij})$ using the steady state analysis of the Markov chain $\pi\mathbf{P} = \pi$ along with the constraint $\sum P(H_{ij}) = 1$, where π (stationary distribution) and $\mathbf{P}$ (transition matrix) are given as

$$\pi = [P(H_{00}), P(H_{01}), P(H_{10}), P(H_{11})],$$

$$\mathbf{P} = \begin{bmatrix} (1-P_{01})\left(1-P_f^{ts}\right) & P_{01}P_m^{ts_c} & \left(1-P_{01}P_f^{ts}\right) & P_{01}(1-P_m^{ts_c}) \\ P_{10}\left(1-P_f^{ts_c}\right) & (1-P_{10})P_m^{ts} & P_{10}P_f^{ts_c} & (1-P_{10})(1-P_m^{ts}) \\ (1-P_{01})\left(1-P_f^{so}\right) & P_{01}P_m^{so_c} & \left(1-P_{01}P_f^{so}\right) & P_{01}(1-P_m^{so_c}) \\ P_{10}\left(1-P_f^{so_c}\right) & (1-P_{10})P_m^{so} & P_{10}P_f^{so_c} & (1-P_{10})(1-P_m^{so}) \end{bmatrix}. \tag{7}$$

After some manipulations, $P(H_{00})$ and $P(H_{01})$ are expressed as:

$$\begin{bmatrix} P(H_{00}) \\ P(H_{01}) \end{bmatrix} = \begin{bmatrix} \frac{(P_{01}+P_{10})(k_1-k_2)}{k_2} & -\frac{(P_{01}+P_{10})k_3}{k_2} \\ k_6 - \frac{k_4 k_1}{k_2} & k_7 + \frac{k_4 k_3}{k_2} \end{bmatrix}^{-1} \times \begin{bmatrix} -P_{10} + \frac{K_6 k_5}{k_2} \\ k_4 - \frac{k_4 k_5}{k_2} \end{bmatrix}, \tag{8}$$

where

$$\begin{aligned} &k_1 = k_5 - (1-P_{01})P_f^{ts}, \quad k_2 = 1 + k_5 - P_f^{so}(1-P_{01}), \\ &k_3 = -k_5 + P_{10}P_f^{ts_c}, \quad k_4 = -P_m^{so}(1-P_{10}) + P_m^{so_c}P_{01}, \\ &k_5 = P_{10}P_f^{so_c}, \quad k_6 = k_4 + P_{01}\left(P_m^{ts_c} - P_m^{so_c}\right), \\ &k_7 = k_4 - 1 - P_m^{so_c}P_{01} + P_m^{ts}(1-P_{01}). \end{aligned} \tag{9}$$

Given $P(H_{00})$ and $P(H_{01})$, we are now ready to calculate the false alarm and miss-detection probabilities. For simplicity, we consider energy-detection based

sensing. With this sensing method, the energy of the received signal is calculated for a specific number of symbols and the result is compared with a threshold to determine whether the channel is busy or free. If $\boldsymbol{y}(n)$ is the received signal at a given SU, the energy is calculated as $M = \frac{1}{f_s \tau_s} \sum_{n=1}^{f_s \tau_s} |\boldsymbol{y}(n)|^2$. By comparing M with a threshold, we can compute the false alarm and miss-detection probabilities of that user as $P_f = Pr[M > \epsilon \mid H_0]$ and $P_m = Pr[M < \epsilon \mid H_1]$.

As we discussed earlier, all SUs perform the sensing and then report their sensing results to the SBS. The SBS makes a cooperative decision on the PU activity. It is clear that SUs may report either their binary decision about presence of PU (hard decision) or their exact energy measurement (soft decision) to the SBS. In the case of hard decision, the SBS applies the k out of n rule, i.e., if k or more SUs decides PU is active, the channel is assumed to be busy. Otherwise the channel is sensed as free. In the case of soft decision, the SBS uses the energy measurements of all the users to make the decision. Therefore, in the following, we calculate the sensing metrics for each user before extending the results to the cooperative sensing metrics using hard and soft decision methods.

3.1 Individual Sensing Performance

To calculate the probabilities of false alarm and miss-detection for each SU, it is noted that SU can be in TS or SO. While working in TS mode, the received signal at i^{th} SU can be written as

$$\boldsymbol{y}_i^{ts}(n) = \begin{cases} \sum_{j=1}^{N} \boldsymbol{h}_{ji}(n)\, \boldsymbol{x}_j(n) + \boldsymbol{u}_i(n), & H_0 \\ \sum_{j=0}^{N} \boldsymbol{h}_{ji}(n)\, \boldsymbol{x}_j(n) + \boldsymbol{u}_i(n), & H_1 \end{cases}, \tag{10}$$

for $i = 1, \ldots, N$. On the other hand, in the SO mode, the SUs do not transmit, and (10) can be simplified to

$$\boldsymbol{y}_i^{so}(n) = \begin{cases} \boldsymbol{u}_i(n), & H_0 \\ \boldsymbol{h}_{0i}(n)\, \boldsymbol{x}_0(n) + \boldsymbol{u}_i(n), & H_1 \end{cases}. \tag{11}$$

Now, as PU activity is non-time slotted, we have two different types of slots:

1. The slots in which the PU activity does not change.
2. The slots in which PU activity status changes.

In the following, we will analyze each of these cases. For that, we shall use M_i^j to denote the energy received at user $i \in \{1, \ldots, N\}$ while working in mode $j \in \{ts, so\}$ and ${}_iP_f^j$ and ${}_iP_m^j$ are the corresponding probabilities of false alarm and miss detection.

The Slots in Which the PU Activity Does Not Change. As SO is a special case of TS, we first find the probabilities of false alarm and miss-detection for user i for the general form in (10) (TS mode). We will then use the results to find ${}_iP_f^{so}$ and ${}_iP_m^{so}$. To this end, we have the following propositions regarding the false-alarm and miss-detection probabilities of TS mode. Their proofs are rather straightforward, and we omit them for the brevity of the presentation.

Proposition 1. *Using the Central Limit Theorem, for the large number of samples ($f_s\tau_s$), the distribution of M_i^{ts} given H_0 can be approximated by Gaussian distribution with the following mean and variance*

$$E\left[M_i^{ts} \mid H_0\right] = \sum_{j=1}^{N} \sigma_{ji}^2 \sigma_j^2 + \sigma_{u_i}^2, \tag{12}$$

$$Var\left[M_i^{ts} \mid H_0\right] = \frac{1}{f_s\tau_s}\left\{\sum_{j=1}^{N} E\left[|\boldsymbol{h}_{ji}(n)|^4\right] E\left[|\boldsymbol{x}_j(n)|^4\right] + 4\sum_{j=1}^{N-1}\sum_{k=j+1}^{N} \sigma_{ji}^2\sigma_{ki}^2\sigma_j^2\sigma_k^2 + \right.$$
$$\left. + E\left[|\boldsymbol{u}_i(n)|^4\right] + 4\sigma_{u_i}^2 \sum_{j=1}^{N} \sigma_{ji}^2\sigma_j^2 - \left(\sum_{j=1}^{N} \sigma_{ji}^2\sigma_j^2 + \sigma_{u_i}^2\right)^2\right\}. \tag{13}$$

Proposition 2. *Using the Central Limit Theorem, for the large number of samples ($f_s\tau_s$), the distribution of M_i^{ts} given H_1 can be approximated by Gaussian distribution with the following mean and variance*

$$E\left[M_i^{ts} \mid H_1\right] = \sum_{j=0}^{N} \sigma_{ji}^2 \sigma_j^2 + \sigma_{u_i}^2, \tag{14}$$

$$Var\left[M_i^{ts} \mid H_1\right] = \frac{1}{f_s\tau_s}\left\{\sum_{j=0}^{N} E\left[|\boldsymbol{h}_{ji}(n)|^4\right] E\left[|\boldsymbol{x}_j(n)|^4\right] + 4\sum_{j=0}^{N-1}\sum_{k=j+1}^{N} \sigma_{ji}^2\sigma_{ki}^2\sigma_j^2\sigma_k^2 + \right.$$
$$\left. + E\left[|\boldsymbol{u}_i(n)|^4\right] + 4\sigma_{u_i}^2 \sum_{j=0}^{N} \sigma_{ji}^2\sigma_j^2 - \left(\sum_{j=0}^{N} \sigma_{ji}^2\sigma_j^2 + \sigma_{u_i}^2\right)^2\right\}. \tag{15}$$

Now, considering that in sensing mode, all SUs are silent. From (11), we can use the results of Propositions 1 and 2 to find the statistics of the received energy at user i in the SO mode M_i^{so} as

$$\mathrm{E}\left[M_i^{so} \mid H_0\right] = \sigma_{u_i}^2, \mathrm{Var}\left[M_i^{so} \mid H_0\right] = \frac{1}{f_s\tau_s}\left(\mathrm{E}\left[|\boldsymbol{u}_i(n)|^4\right] - \sigma_{u_i}^4\right), \tag{16}$$

$$\mathrm{E}\left[M_i^{so} \mid H_1\right] = \sigma_{u_i}^2 + \sigma_{0i}^2\sigma_0^2, \tag{17}$$

$$\mathrm{Var}\left[M_i^{so} \mid H_1\right] = \frac{1}{f_s\tau_s}\left(\mathrm{E}\left[|\boldsymbol{h}_{0i}(n)|^4\right]\mathrm{E}\left[|\boldsymbol{x}_0(n)|^4\right] + \mathrm{E}\left[|\boldsymbol{u}_i(n)|^4\right] - \left(\sigma_{0i}^2\sigma_0^2 - \sigma_{u_i}^2\right)^2\right). \tag{18}$$

As a result, the sensing metrics for user i are calculated as

$${}_iP_f^j = Q\left(\frac{\epsilon_i^j - \mathrm{E}\left[M_i^j \mid H_0\right]}{\sqrt{\mathrm{Var}\left[M_i^j \mid H_0\right]}}\right), {}_iP_m^j = 1 - Q\left(\frac{\epsilon_i^j - \mathrm{E}\left[M_i^j \mid H_1\right]}{\sqrt{\mathrm{Var}\left[M_i^j \mid H_1\right]}}\right), \tag{19}$$

for $j \in \{ts, so\}$ and $i = 1, \ldots, N$.

The Slots in Which PU Activity Status Changes. In this case, define two random variables $\hat{T}_1$ and $\hat{T}_0$ as the forward recurrence time for the ON and OFF periods of PU, respectively, which are observed at the sensing decision time. It can then be verified that the probability distributions of these two random variables are:

$$f_{\hat{T}_1}(t) = \frac{\int_t^\infty f_{T_1}(x)\,dx}{\tau_1}, f_{\hat{T}_0}(t) = \frac{\int_t^\infty f_{T_0}(x)\,dx}{\tau_0}. \tag{20}$$

The average forward recurrence time for ON and OFF periods of the slots with PU activity being changed are therefore calculated as

$$\mu_{\hat{T}_i} = \mathrm{E}\left[\hat{T}_i \mid \hat{T}_i < \tau_s\right] = \frac{\int_0^{\tau_s} t f_{\hat{T}_i}(t)\,dt}{F_{\hat{T}_i}(\tau_s)} = \frac{\int_0^{\tau_s} t\left[\int_t^\infty f_{T_i}(x)\,dx\right]dt}{\int_0^{\tau_s}\left[\int_t^\infty f_{T_i}(x)\,dx\right]dt}, \tag{21}$$

where $F(\cdot)$ denotes the cumulative distribution function (CDF).

Now, assuming that PU status changes after $\mu_{\hat{T}_i}$ seconds from the start of the frame. This is a reasonable assumption, as these slots rarely happen. While working in mode j, $j \in \{ts, so\}$, the energy received at i^{th} SU when PU status changes from ON to OFF, $M_i^j \mid H_1 \to H_0$, and OFF to ON, $M_i^j \mid H_0 \to H_1$, can then be expressed as

$$M_i^j \mid H_1 \to H_0 = \frac{1}{f_s\tau_s}\left[\sum_{n=1}^{f_s\mu_{\hat{T}_1}}\left|\left[\boldsymbol{y}_i^j(n) \mid H_1\right]\right|^2 + \sum_{n=f_s\mu_{\hat{T}_1}+1}^{f_s\tau_s}\left|\left[\boldsymbol{y}_i^j(n) \mid H_0\right]\right|^2\right], \tag{22}$$

$$M_i^j \mid H_0 \to H_1 = \frac{1}{f_s\tau_s}\left[\sum_{n=1}^{f_s\mu_{\hat{T}_0}}\left|\left[\boldsymbol{y}_i^j(n) \mid H_0\right]\right|^2 + \sum_{n=f_s\mu_{\hat{T}_0}+1}^{f_s\tau_s}\left|\left[\boldsymbol{y}_i^j(n) \mid H_1\right]\right|^2\right]. \tag{23}$$

Using Central Limit Theorem, Levy-Cramer Theorem, Propositions 1 and 2, the results in (16–18), we then have:

$$\mathrm{E}\left[M_i^j \mid H_k \to H_{1-k}\right] = \frac{1}{\tau_s}\left\{\mu_{\hat{T}_k}\mathrm{E}\left[M_i^j \mid H_k\right] + \left(\tau_s - \mu_{\hat{T}_k}\right)\mathrm{E}\left[M_i^j \mid H_{1-k}\right]\right\}, \tag{24}$$

$$\mathrm{Var}\left[M_i^j \mid H_k \to H_{1-k}\right] = \frac{1}{\tau_s}\left\{\mu_{\hat{T}_k}\mathrm{Var}\left[M_i^j \mid H_k\right] + \left(\tau_s - \mu_{\hat{T}_k}\right)\mathrm{Var}\left[M_i^j \mid H_{1-k}\right]\right\}, \tag{25}$$

where $k = 0, 1$. That leads to the sensing metrics of i^{th} SU working in mode j of the slots that PU activity changes as:

$${}_iP_f^{j_c} = Q\left(\frac{\epsilon_i^{j_c} - \mathrm{E}\left[M_i^j \mid H_1 \to H_0\right]}{\sqrt{\mathrm{Var}\left[M_i^j \mid H_1 \to H_0\right]}}\right),\ {}_iP_m^{j_c} = 1 - Q\left(\frac{\epsilon_i^{j_c} - \mathrm{E}\left[M_i^j \mid H_0 \to H_1\right]}{\sqrt{\mathrm{Var}\left[M_i^j \mid H_0 \to H_1\right]}}\right). \tag{26}$$

Note that we use the sub-index c to refer to the change of PU status.

3.2 Global (Cooperative) Sensing Performance

In this subsection, the focus is on the global sensing metrics. We shall first consider the hard decision based metrics before examining the soft decision ones.

Hard Decision. As we mentioned before, the global decision rule is implemented as k out of n rule. This rule includes simpler methods such as OR, AND and Majority rules as specific cases.

Let the set $\mathcal{S} = \{1, 2, 3, \ldots N\}$ represent the SUs. Also let $\mathcal{P}_k(\mathcal{S})$ be the set containing all subsets of $\mathcal{S}$ having k or more elements. By assuming that all decisions are independent, the global false alarm and miss detection probabilities based on the k out of n rule are

$$P_f^j = \sum_{\mathcal{A} \in \mathcal{P}_k(\mathcal{S})} \prod_{i \in \mathcal{A}} {}_iP_f^j \prod_{i \in \bar{\mathcal{A}}} \left(1 - {}_iP_f^j\right), \tag{27}$$

and

$$P_m^j = 1 - \sum_{\mathcal{A} \in \mathcal{P}_k(\mathcal{S})} \prod_{i \in \mathcal{A}} \left(1 - {}_iP_m^j\right) \prod_{i \in \bar{\mathcal{A}}} {}_iP_m^j, \tag{28}$$

where $j \in \{ts, so, ts_c, so_c\}$ and $\bar{\mathcal{A}}$ is the complement of $\mathcal{A}$. Now, let consider the three special cases of OR, AND and Majority rules.

OR Rule. The SBS decides that PU is active if one or more SUs determine that PU is busy ($k = 1$).

$$P_f^j = 1 - \prod_{i=1}^{N} \left(1 - {}_iP_f^j\right) \text{ and } P_m^j = \prod_{i=1}^{N} {}_iP_m^j. \tag{29}$$

AND Rule. The SBS decides that PU is active if all SUs sense the channel busy ($k = N$).

$$P_f^j = \prod_{i=1}^{N} {}_iP_f^j \text{ and } P_m^j = 1 - \prod_{i=1}^{N} \left(1 - {}_iP_m^j\right). \tag{30}$$

Majority Rule. If more than half of SUs detect PU activity, the SBS decides that PU is active. So, the probabilities of false alarm and miss detection for majority rule can be obtained from (27) and (28) by setting $k = \lceil \frac{N}{2} \rceil$.

Soft Decision. For soft decision, the SBS decides the vacancy of the channel based on the following metric $M^j = \sum_{i=1}^{N} M_i^j, \quad j \in \{ts, so\}$. Since M_i^j is Gaussian, the mean and variance of M^j under different hypothesis settings are

$$\mathrm{E}\left[M^j \mid \mathcal{H}\right] = \sum_{i=1}^{N} \mathrm{E}\left[M_i^j \mid \mathcal{H}\right], \mathrm{Var}\left[M^j \mid \mathcal{H}\right] = \sum_{i=1}^{N} \mathrm{Var}\left[M_i^j \mid \mathcal{H}\right], \tag{31}$$

for $j \in \{ts, so\}$ and $\mathcal{H} \in \{H_0, H_1, H_1 \to H_0, H_0 \to H_1\}$. As a result, P_f and P_m under the soft decision based method are calculated as

$$P_f^j = Q\left(\frac{\epsilon^j - \mathrm{E}\left[M^j \mid H_0\right]}{\sqrt{\mathrm{Var}\left[M^j \mid H_0\right]}}\right), \quad P_f^{j_c} = Q\left(\frac{\epsilon^j - \mathrm{E}\left[M^j \mid H_1 \to H_0\right]}{\sqrt{\mathrm{Var}\left[M^j \mid H_1 \to H_0\right]}}\right), \tag{32}$$

$$P_m^j = 1 - Q\left(\frac{\epsilon^j - \mathrm{E}\left[M^j \mid H_1\right]}{\sqrt{\mathrm{Var}\left[M^j \mid H_1\right]}}\right), \quad P_m^{j_c} = 1 - Q\left(\frac{\epsilon^j - \mathrm{E}\left[M^j \mid H_0 \to H_1\right]}{\sqrt{\mathrm{Var}\left[M^j \mid H_0 \to H_1\right]}}\right). \tag{33}$$

4 Rate Region and Achievable Rates

Given that the random variables α and β and the sensing perfomance metrics have been fully characterized in the previous section, we will analyze the rate region and the achievable rate of each SU under NOMA with SIC in this section. To simplify the notations, hereafter, the use of $\boldsymbol{x} = x_1 + ix_2$ and $\boldsymbol{x} = [x_1, x_2]$ to indicate a 2-D vector is interchangeable.

4.1 Rate Region

The main results regarding the rate region are stated in the following proposition.

Proposition 3. *The convex hull of all* $\{R_j\}_{j=1}^N$ *satisfying*

$$R_j \leq P\left(\beta = 1\right)\left\{E_{\boldsymbol{h}_{jr}}\left[\Gamma_G\left(\left|\boldsymbol{h}_{jr}\right|^2 \sigma_j^2\right)\right] - \Gamma_G\left(0\right)\right\}, \tag{34}$$

$$\sum_{j=1}^{N} R_j \leq P\left(\beta = 1\right)\left\{E_{\vec{\boldsymbol{h}}_r}\left[\Gamma_G\left(\sum_{j=1}^{N}\left|\boldsymbol{h}_{jr}\right|^2 \sigma_j^2\right)\right] - \Gamma_G\left(0\right)\right\}, \tag{35}$$

is an achievable rate region, where

$$\Gamma_G\left(v\right) = -\log\left(\sum_{i=1}^{p+1}\frac{\epsilon_{z,i}}{\pi\left(\sigma_{z,i}^2 + v\right)}\right) + \frac{\left(\sum_{i=1}^{p+1}\frac{\epsilon_{z,i}}{2}\left(\sigma_{z,i}^2 + v\right)\right)\left(\sum_{i=1}^{p+1}\frac{\epsilon_{z,i}}{\pi\left(\sigma_{z,i}^2+v\right)^2}\right)}{\sum_{i=1}^{p+1}\frac{\epsilon_{z,i}}{\pi\left(\sigma_{z,i}^2+v\right)}}, \tag{36}$$

and $\vec{\boldsymbol{h}}_r = [\boldsymbol{h}_{1r}, \boldsymbol{h}_{2r}, \cdots, \boldsymbol{h}_{Nr}]$.

Proof. Let's first write the achievable rates in terms of mutual information between $\boldsymbol{y}_r$ and the user input signals as:

$$R_j \leq P\left(\beta = 1\right)\mathrm{E}_{\vec{\boldsymbol{h}}_r}\left[I\left(\boldsymbol{x}_j; \boldsymbol{y}_r^{\beta} \mid \{\boldsymbol{x}_k\}_{k=1,k\neq j}^{N}, \vec{\boldsymbol{h}}_r\right)\right], \tag{37}$$

and

$$\sum_{j=1}^{N} R_j \leq P\left(\beta=1\right) \mathrm{E}_{\vec{\boldsymbol{h}}_r}\left[I\left(\{\boldsymbol{x}_k\}_{k=1}^{N}; \boldsymbol{y}_r^{\beta} \mid \vec{\boldsymbol{h}}_r\right)\right]. \tag{38}$$

We then expand $I\left(\boldsymbol{x}_j; \boldsymbol{y}_r^{\beta} \mid \{\boldsymbol{x}_k\}_{k=1,k\neq j}^{N}, \vec{\boldsymbol{h}}_r\right)$ as:

$$\mathrm{H}\left(\boldsymbol{y}_r^{\beta} \mid \{\boldsymbol{x}_k\}_{k=1,k\neq j}^{N}, \vec{\boldsymbol{h}}_r\right) - \mathrm{H}\left(\boldsymbol{y}_r^{\beta} \mid \{\boldsymbol{x}_k\}_{k=1}^{N}, \vec{\boldsymbol{h}}_r\right) = \mathrm{H}\left(\boldsymbol{h}_{jr}\boldsymbol{x}_j + \boldsymbol{z}_{\beta} \mid \boldsymbol{h}_{jr}\right) - \mathrm{H}\left(\boldsymbol{z}_{\beta}\right). \tag{39}$$

It is clear that by calculating $\mathrm{H}\left(\boldsymbol{h}_{jr}\boldsymbol{x}_j + \boldsymbol{z}_{\beta} \mid \boldsymbol{h}_{jr}\right)$ and setting $\boldsymbol{h}_{jr} = 0$, $\mathrm{H}\left(\boldsymbol{z}_{\beta}\right)$ can be obtained. In particular, we know that the PDF of $\boldsymbol{r}_j = \boldsymbol{h}_{jr}\boldsymbol{x}_j + \boldsymbol{z}_{\beta}$ given $\boldsymbol{h}_{jr}$ is given as $f_{R_j|H_{jr}}\left(\boldsymbol{y}\right) = \sum_{i=1}^{p+1} \epsilon_{z,i}\mathcal{CN}(\boldsymbol{y}, 0, \sigma_{z,i}^2 + \left|\boldsymbol{h}_{jr}\right|^2 \sigma_j^2)$.. Hence,

$$\mathrm{H}\left(\boldsymbol{h}_{jr}\boldsymbol{x}_j + \boldsymbol{z}_{\beta} \mid \boldsymbol{h}_{jr}\right) = -\sum_{i=1}^{p+1} \int_{\mathbb{R}} \epsilon_{z,i}\mathcal{CN}(\boldsymbol{y}, 0, \sigma_{z,i}^2 + \left|\boldsymbol{h}_{jr}\right|^2 \sigma_j^2) \log\left(f_{R_j|H_{jr}}\left(\boldsymbol{y}\right)\right) d\boldsymbol{y}. \tag{40}$$

There is no closed form solution of (40) due to the logarithm of a sum of Gaussian distributions [5,6]. In the following, our approach is to find an approximation achieving an arbitrary level of accuracy for the entropy of GM distribution using Taylor series expansion. Specifically, we use Taylor series to expand $\log\left(f_{R_j|H_{jr}}\left(\boldsymbol{y}\right)\right)$ over the mean vector of each Gaussian component which is 0 in this case. Thus, we have

$$\begin{aligned}&\mathrm{H}\left(\boldsymbol{h}_{jr}\boldsymbol{x}_j + \boldsymbol{z}_{\beta} \mid \boldsymbol{h}_{jr}\right) = \\ &-\sum_{i=1}^{p+1} \int_{\mathbb{R}} \epsilon_{z,i}\mathcal{CN}(\boldsymbol{y}, 0, \sigma_{z,i}^2 + \left|\boldsymbol{h}_{jr}\right|^2 \sigma_j^2) \sum_{|\alpha|\leq d} \frac{D^{\alpha} \log\left(f_{R_j|H_{jr}}\left(\boldsymbol{y}\right)\right)|_{\boldsymbol{y}=0}}{\alpha!} \boldsymbol{y}^{\alpha} d\boldsymbol{y},\end{aligned} \tag{41}$$

where $|\alpha| = \alpha_1 + \alpha_2$, $\alpha! = \alpha_1!\alpha_2!$, $\boldsymbol{y}^{\alpha} = y_1^{\alpha_1} y_2^{\alpha_2}$, and $D^{\alpha} f\left(\boldsymbol{y}\right) = \frac{\partial^{|\alpha|} f(\boldsymbol{y})}{\partial y_1^{\alpha_1} \partial y_2^{\alpha_2}}$. Moreover, d is chosen based on the level of accuracy. It then follows that

$$\begin{aligned}&\mathrm{H}\left(\boldsymbol{h}_{jr}\boldsymbol{x}_i + \boldsymbol{z}_{\beta} \mid \boldsymbol{h}_{jr}\right) = -\sum_{i=1}^{p+1} \sum_{\substack{|\alpha|\leq d \\ \alpha_1,\alpha_2\in\mathcal{A}_e}} \\ &\epsilon_{z,i} \frac{D^{\alpha} \log\left(f_{R_j|H_{jr}}\left(\boldsymbol{y}\right)\right)\big|_{\boldsymbol{y}=0}}{\alpha!} \left(\frac{\sigma_{z,i}^2 + \left|\boldsymbol{h}_{jr}\right|^2 \sigma_j^2}{2}\right)^{|\alpha|/2} (\alpha_1 - 1)!!\,(\alpha_2 - 1)!!,\end{aligned} \tag{42}$$

where $\mathcal{A}_e$ denotes the set of even natural numbers and $a!! = a\,(a-2)\,(a-4)\cdots 1$. As we will demonstrate shortly, the use of $d = 3$ can result in a highly accurate approximation. In this case, we have $\mathrm{H}\left(\boldsymbol{h}_{jr}\boldsymbol{x}_i + \boldsymbol{z}_{\beta} \mid \boldsymbol{h}_{jr}\right)$ as

$$-\log\left(f_{R_j|H_{jr}}\left(\boldsymbol{y}\right)\right)|_{\boldsymbol{y}=0}-\sum_{i=1}^{p+1}\epsilon_{z,i}\left[\frac{\partial^2\log\left(f_{R_j|H_{jr}}\left(\boldsymbol{y}\right)\right)}{\partial y_1^2}\right]\Big|_{\boldsymbol{y}=0}\frac{\sigma_{z,i}^2+\left|\boldsymbol{h}_{jr}\right|^2\sigma_j^2}{2}. \tag{43}$$

Here, we have used the fact that $f_{R_j|H_{jr}}\left(\boldsymbol{y}\right)$ is symmetric with respect to y_1 and y_2, i.e., $\frac{\partial^2\log\left(f_{R_j|H_{jr}}(\boldsymbol{y})\right)}{\partial y_1^2}\big|_{\boldsymbol{y}=0}=\frac{\partial^2\log\left(f_{R_j|H_{jr}}(\boldsymbol{y})\right)}{\partial y_2^2}\big|_{\boldsymbol{y}=0}$. After some simple manipulations, we obtain

$$R_j\leq P\left(\beta=1\right)\left\{\mathrm{E}_{\boldsymbol{h}_{jr}}\left[\Gamma_G\left(\left|\boldsymbol{h}_{jr}\right|^2\sigma_j^2\right)\right]-\Gamma_G\left(0\right)\right\}, \tag{44}$$

where

$$\Gamma_G\left(v\right)=-\log\left(\sum_{i=1}^{p+1}\frac{\epsilon_{z,i}}{\pi\left(\sigma_{z,i}^2+v\right)}\right)+\frac{\left(\sum_{i=1}^{p+1}\frac{\epsilon_{z,i}}{2}\left(\sigma_{z,i}^2+v\right)\right)\left(\sum_{i=1}^{p+1}\frac{\epsilon_{z,i}}{\pi\left(\sigma_{z,i}^2+v\right)^2}\right)}{\sum_{i=1}^{p+1}\frac{\epsilon_{z,i}}{\pi\left(\sigma_{z,i}^2+v\right)}}. \tag{45}$$

Finally, the sum-rate can be calculated using the following PDF of $\boldsymbol{y}_r^{\beta}$

$$f_{Y_r|\vec{H}_r}\left(\boldsymbol{y}\right)=\sum_{i=1}^{p+1}\epsilon_{z,i}\mathcal{CN}(\boldsymbol{y},0,\sigma_{z,i}^2+\sum_{j=1}^{N}\left|\boldsymbol{h}_{jr}\right|^2\sigma_j^2). \tag{46}$$

Then following the same procedure in obtaining (44) earlier, we have

$$\sum_{j=1}^{N}R_j\leq P\left(\beta=1\right)\left\{\mathrm{E}_{\vec{\boldsymbol{h}}_r}\left[\Gamma_G\left(\sum_{j=1}^{N}\left|\boldsymbol{h}_{jr}\right|^2\sigma_j^2\right)\right]-\Gamma_G\left(0\right)\right\}. \tag{47}$$

4.2 Achievable Rates of SUs

Based on the SIC NOMA described earlier, the received signal to decode the information of the j^{th} user under SIC is given $\boldsymbol{y}_{r,j}^{\beta}=\sum_{k=j}^{N}\boldsymbol{h}_{kr}\boldsymbol{x}_k+\boldsymbol{z}_{\beta}$. By treating the signal of k^{th} user with $k>j$ as noise for user j, we can write the achievable rate of j^{th} user as

$$\begin{aligned}R_j&=P\left(\beta=1\right)\mathrm{E}_{\vec{\boldsymbol{h}}_r}\left[I\left(\boldsymbol{x}_j;\boldsymbol{y}_{r,j}^{\beta}\mid\vec{\boldsymbol{h}}_r\right)\right]\\&=P\left(\beta=1\right)\mathrm{E}_{\vec{\boldsymbol{h}}_r}\left[\mathrm{H}\left(\sum_{k=j}^{N}\boldsymbol{h}_{kr}\boldsymbol{x}_k+\boldsymbol{z}_{\beta}\mid\vec{\boldsymbol{h}}_r\right)-\mathrm{H}\left(\sum_{k=j+1}^{N}\boldsymbol{h}_{kr}\boldsymbol{x}_k+\boldsymbol{z}_{\beta}\mid\vec{\boldsymbol{h}}_r\right)\right].\end{aligned} \tag{48}$$

Using the same procedure that we found $\mathrm{H}\left(\boldsymbol{y}_r^{\beta}\mid\vec{\boldsymbol{h}}_r\right)$ in (47), we obtain

$$\mathrm{H}\left(\sum_{k=j}^{N}\boldsymbol{h}_{kr}\boldsymbol{x}_k+\boldsymbol{z}_{\beta}\mid\vec{\boldsymbol{h}}_r\right)=\Gamma_G\left(\sum_{k=j}^{N}\left|\boldsymbol{h}_{kr}\right|^2\sigma_j^2\right). \tag{49}$$

Note that $\mathrm{H}\left(\sum_{k=j+1}^{N} \boldsymbol{h}_{jr}\boldsymbol{x}_j + \boldsymbol{z}_\beta \mid \vec{\boldsymbol{h}}_r\right)$ can be calculated using Taylor expansion. Finally, we can calculate the achievable rate R_j as

$$R_j = P\left(\beta = 1\right) \mathrm{E}_{\vec{\boldsymbol{h}}_r}\left[\Gamma_G\left(\sum_{k=j}^{N} \left|\boldsymbol{h}_{kr}\right|^2 \sigma_k^2\right) - \Gamma_G\left(\sum_{k=j+1}^{N} \left|\boldsymbol{h}_{kr}\right|^2 \sigma_k^2\right)\right]. \quad (50)$$

5 Numerical Result

In this section, numerical results are provided to support our previous analysis and derivations. We use the sampling frequency of 1 MHz and the duration of each SU slot is assumed to be 1 ms. Moreover, T_1 and T_0 are modeled as exponential random variables with mean 100 ms. $\boldsymbol{u}$, $\boldsymbol{w}$ and fading coefficients are modeled as circularly symmetric Gaussian random variables with mean zero and variances per dimension 0.2, 0.3 and 1, respectively. For simplicity, we consider a 2-user channel. However, we would like to note that our results apply to any number of users. For the 2-user case, we assume both users use the same power σ. The sensing is performed using the soft decision method. While our analysis holds for any input signaling scheme, we will focus Gaussian input signals. In all simulations, SNR is defined as $\mathrm{SNR} = \frac{\sigma^2}{\sigma_u^2}$.

In Fig. 2, we plot the rate regions of a two-user secondary network at SNR = 5 dB. Note that the rate region is calculated from (37) and (38) using Taylor expansion with $k = 3$. For comparison, the rate regions obtained by numerical integration are also provided. It can be seen from Fig. 2 that $k = 3$ provides accurate results that are very close to the numerical calculations. Note that the symmetry of the rate region comes from the fact that both users have the same power.

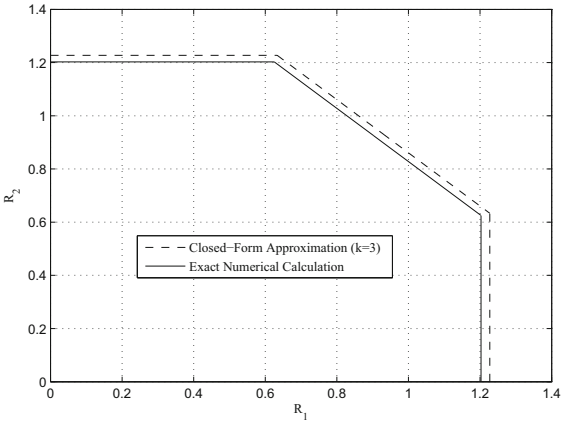

Fig. 2. Rate region of a 2-user channel using Gaussian input signals.

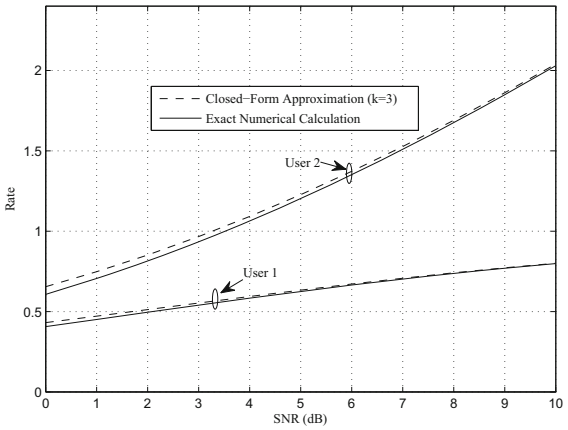

Fig. 3. The achievable rates with Gaussian signals.

In Fig. 3, the achievable rates versus SNR with SIC decoding for the two users are presented. Again, the accuracy of the closed-form approximations is clearly observed. Note that user 1 achieves a lower rate than user 2. This is because user 1 is assumed to be the first user to be detected. The fairness can certainly be improved by allocating power proportionally to the users.

6 Conclusion

This paper investigated the rate region and the achievable rates of a NOMA FD CR channel. Under the assumption of imperfect SIS and spectrum sensing, the sensing performance was first analyzed. Our method relied on a Markov chain model to combine the sensing results under different sensing scenarios and obtain the probability of collision between the SUs and PU. Due to the difficulty in obtaining the explicit expressions of the channel capacity and mutual information in GM, we then propose new closed-form approximations of the rate region and the achievable rate for each of the users with arbitrarily small errors. The rate region and the achievable rates were then established.

References

1. Afifi, W., Krunz, M.: Incorporating self-interference suppression for full-duplex operation in opportunistic spectrum access systems. IEEE Trans. Wireless Commun. **14**(4), 2180–2191 (2015). https://doi.org/10.1109/TWC.2014.2382124
2. Ali, M.S., Tabassum, H., Hossain, E.: Dynamic user clustering and power allocation for uplink and downlink non-orthogonal multiple access (NOMA) systems. IEEE Access **4**, 6325–6343 (2016). https://doi.org/10.1109/ACCESS.2016.2604821
3. Di, B., Song, L., Li, Y.: Sub-channel assignment, power allocation, and user scheduling for non-orthogonal multiple access networks. IEEE Trans. Wireless Commun. **15**(11), 7686–7698 (2016). https://doi.org/10.1109/TWC.2016.2606100

4. Dinc, T., Chakrabarti, A., Krishnaswamy, H.: A 60 GHz CMOS full-duplex transceiver and link with polarization-based antenna and RF cancellation. IEEE J. Solid-State Circuits **51**(5), 1125–1140 (2016)
5. Durrieu, J.L., Thiran, J.P., Kelly, F.: Lower and upper bounds for approximation of the Kullback-Leibler divergence between Gaussian mixture models. In: ICASSP, IEEE International Conference on Acoustics, Speech and Signal Processing - Proceedings (Mc), pp. 4833–4836 (2012). https://doi.org/10.1109/ICASSP.2012.6289001
6. Hershey, J.R., Olsen, P.A.: Approximating the Kullback-Leibler divergence between Gaussian mixture models. Acoust. Speech Signal Process. **4**(6), IV–317 (2007)
7. Hossain, E., Niyato, D., Han, Z.: Dynamic Spectrum Access and Management in Cognitive Radio Networks. Cambridge University Press, Cambridge (2009)
8. Kim, D., Lee, H., Hong, D.: A survey of in-band full-duplex transmission: from the perspective of PHY and MAC layers. IEEE Commun. Surv. Tutor. **17**(4), 2017–2046 (2015)
9. Liao, Y., Wang, T., Song, L., Han, Z.: Listen-and-talk: protocol design and analysis for full-duplex cognitive radio networks. IEEE Trans. Veh. Technol. **66**(1), 656–667 (2016). https://doi.org/10.1109/TVT.2016.2535483
10. Ozcan, G., Gursoy, M.C., Gezici, S.: Error rate analysis of cognitive radio transmissions with imperfect channel sensing. IEEE Trans. Wireless Commun. **13**(3), 1642–1655 (2014)
11. Ozcan, G., Gursoy, M.C., Gezici, S.: Error rate analysis of cognitive radio transmissions with imperfect channel sensing. IEEE Trans. Wireless Commun. **13**, 1642–1655 (2014). http://arxiv.org/abs/1310.1822
12. Ranjbar, M., Tran, N.H., Nguyen, T., Gursoy, M.C.: Capacity-achieving signals for point-to-point and multiple-access channels under non-Gaussian noise and peak power constraint. IEEE Access **6**, 30977–30989 (2018)
13. Ranjbar, M., Nguyen, H.L., Tran, N.H., Karacolak, T., Sastry, S., Nguyen, L.D.: Energy efficiency of full-duplex cognitive radio in low-power regimes under imperfect spectrum sensing. Mob. Netw. Appl. **26**(4), 1750–1764 (2021). https://doi.org/10.1007/s11036-021-01755-z
14. Vu, H.V., Tran, N.H., Gursoy, M.C., Le-Ngoc, T., Hariharan, S.: Capacity-achieving input distributions of additive quadrature Gaussian mixture noise channels. IEEE Trans. Commun. **63**(10), 3607–3620 (2015)
15. Yang, Z., Ding, Z., Fan, P., Al-Dhahir, N.: The impact of power allocation on cooperative non-orthogonal multiple access networks with SWIPT. IEEE Trans. Wireless Commun. **16**(7), 4332–4343 (2017). https://doi.org/10.1109/TWC.2017.2697380